Proceedings World Geothermal Congress 2020+1
Reykjavik, Iceland, April - October 2021

Present Geothermal Fields of the Chagan Depression in the Yingen-Ejinaqi Basin, Inner Mongolia, Central China

Yinhui Zuo[1,3], Shu Jiang[2,3,*], Qingqing Hao[4], Yongshui Zhou[5]

1. State Key Laboratory of Oil and Gas Geology and Exploitation, Chengdu University of Technology, Chengdu 610059, China

2. Key Lab of Tectonics and Petroleum Resource of Educational Ministry & Faculty of Earth Resources, China University of Geosciences, Wuhan 430074, China

3. Energy & Geoscience Institute, University of Utah, Salt Lake City, UT 84108, USA

4. Research Institute of Mineral Resources, China Metallurgical Geology Bureau, Beijing 101300, China

5. Research Institute of Exploration and Development, Zhongyuan Oilfield, SINOPEC, Puyang 457001, China <Address style>

E-mail address: jiangsu@cug.edu.cn

Keywords: Present geothermal fields; Chagan Depression; Rock thermal conductivity; Terrestrial heat flow; System steady-state temperature.

ABSTRACT

The study of geothermal fields in a basin is significant for the evaluation of petroleum and geothermal resources, and can also provide insights for basin dynamics and tectonic-thermal evolution. This work tests rock thermal conductivity of the Cretaceous Chagan Depression in the Inner Mongolia, central China. The geothermal gradient of four wells is calculated and four terrestrial heat flow data are generated for the first time in the Yingen-Ejinaqi Basin. The results show that the rock thermal conductivity of the Bayingebi 1 and 2 Formations is high, with an average value of 2.38 and 2.33 W/m·K, respectively. The Suhongtu 1 and 2 Formations contain certain magmatic rocks, and the thermal conductivity of magmatic rocks is relatively low. As a result, their thermal conductivity is relatively low, with an average value of 1.78 and 2.21 W/m·K, respectively. The Yingen Formation has a shallow burial depth, with loose rocks and large porosity, and the rock thermal conductivity is relatively low as only 1.85 W/m·K. A total of 193 systematic steady-state temperature measurement data were obtained for the wells X2, X5, Y5 and Y7. The Cenozoic strata are affected by solar radiation, groundwater disturbance and other factors, which are not considered in the calculation. The relationship between temperature and depth indicates that it can be divided into three intervals, and the average geothermal gradients from the upper section to the lower section are 28.9, 37.6 and 27.6 °C/km, respectively. The terrestrial heat flow of the four wells was also calculated by the thermal resistance method with the rock thermal conductivity and geothermal gradient data. The terrestrial heat flow of the Wuliji fault nose structural belt ranges between 61.0 and 81.0 mW/m^2, with an average value of 70.9 mW/m^2, and that of the central uplift belt ranges from 65.1 to 69.2 mW/m^2, with an average value of 67.6 mW/m^2. The average terrestrial heat flow of the Chagan Depression is 70.6 mW/m^2, which is higher than that of the global continent (averaged at 63 mW/m^2), indicating a high geothermal background in the Chagan Depression.

1. INTRODUCTION

The present geothermal fields can provide evidence for a dynamic mechanism and tectonic-thermal evolution, and can also guide petroleum and geothermal resource evaluation (Wang, 2015; Artemieva, 2018; Majorowicz at al., 2019). The Chagan Depression is an important structural feature for oil and gas in the Yingen-Ejinaqi (YE) Basin of Inner Mongolia, and the YE Basin is located at the intersection of the Paleo-Asian Ocean and the Tethys Ocean (Ren, 1999; Wan, 2011). Further, the YE Basin is located in the complex intersection zone of the North China Craton, Tarim Block, Siberian Block, Tianshan-Xing'an orogenic system and Qinling - Qilianshan - Kunlun orogenic system (Ren, 1999; Wei et al., 2006; Wan, 2011; Zhong et al., 2014; Lu et al., 2017) (Figure 1). This region is therefore an ideal place to study many fundamental geological and tectonic problems including present geothermal fields and deep dynamic mechanisms.

The Chagan Depression has been estimated to have a low heat flow value due to the absence of terrestrial heat flow data, mainly distributed between 45 mW/m^2 and 55 mW/m^2 (Wang and Huang, 1988, 1990; Hu et al., 2000). However, these estimated heat flows are based on unsteady-state temperature logging and formation-testing temperature from 9 wells in the Chagan Depression which yielded an average of 74.5 mW/m^2 (Zuo et al., 2013, 2015). To verify whether this depression has high heat flow, system steady-state temperature measurements were carried out during 2016 by a joint team including Chengdu University of Technology, Xi'an Jiaotong University, the Institute of Geology and Geophysics of Chinese Academy of Sciences and Zhongyuan Oilfield, SINOPEC. The system steady-state temperature data (SSSTD) from 193 measurements in Wells X2, X5, Y5 and Y7 were obtained, and 169 rock thermal conductivity data and 90 heat production rate data were tested. This dataset provides a robust estimate of terrestrial heat flow and the LTS of the Chagan Depression.

In this study, the geothermal gradient and terrestrial heat flow in the Chagan Depression are calculated, and the influencing factors of geothermal gradient and tectonic evolution background of geothermal flow are discussed. The results may provide geothermal information for the evaluation of petroleum and geothermal resources in the Chagan Depression.

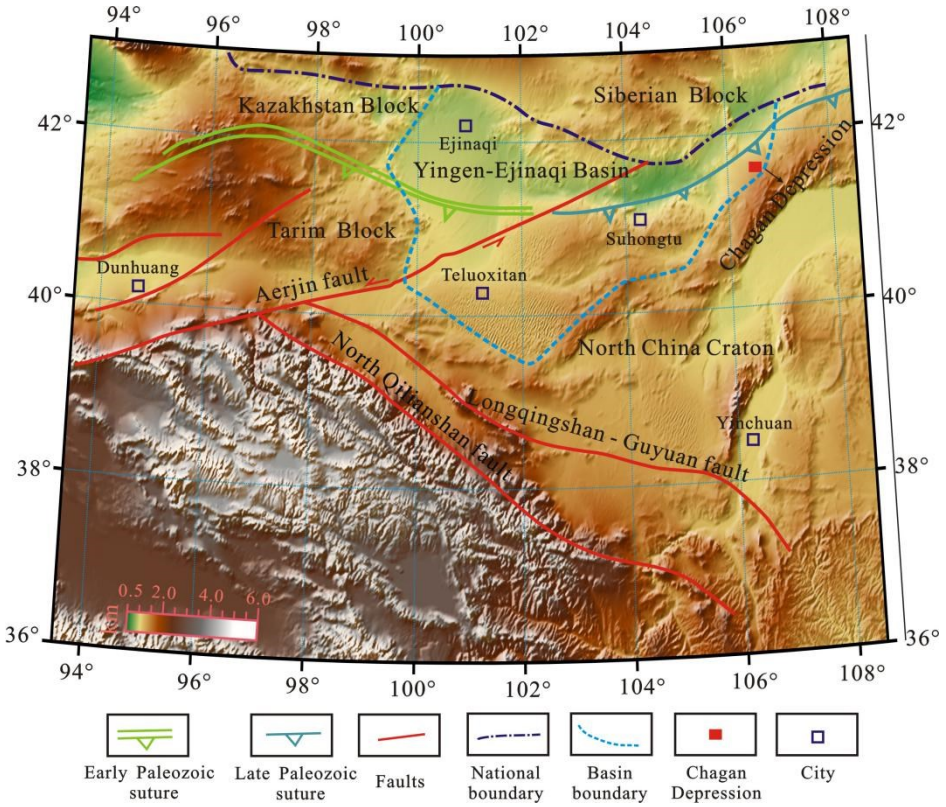

Figure 1: Regional structural and location map of the Chagan Depression (modified from Zhong et al., 2014; the topographic contour employs ETOPO 1 data from the National Geophysical Data Center).

2. GEOLOGICAL SETTINGS

The Chagan Depression is located in the central Chagandelesu subbasin in the eastern YE Basin. It is a Cretaceous rift basin on the folded Late Paleozoic basement (Wang et al., 2016; Zuo et al., 2017). The Chagan Depression witnessed multiple and diverse tectonic activities. The faults in the depression are oriented mainly in the northeast-southwest direction. The Chagan Depression is composed of the western subdepression, the Maotun uplift and the eastern subdepression (Figures 2a, b). The strata in this area are represented by the Early Cenozioc Bayingebi, Suhongtu and Yingen Formations, Late Cenozoic Wulansuhai Formation and other Cenozoic deposits (Figure 2c). The thickness of sedimentary cover in the western subdepression is significantly greater than that of the eastern subdepression. The thickness reaches 5500 m in the central Ehen sag in the western subdepression, whereas the maximum thickness is only 3500 m in the northern central part of the Hantamiao sag zone along the eastern subdepression.

3. METHODS AND PRINCIPLES

3.1 Terrestrial heat flow and geothermal gradient calculation methods

Terrestrial heat flow is a comprehensive parameter reflecting the characteristics of a regional thermal regime. Under the condition of one-dimensional steady-state heat conduction, heat flow can be calculated from the geothermal gradient and rock thermal conductivity Equation 1.

$$q_0 = -K \times G \tag{1}$$

where q_0 is the terrestrial heat flow, mW/m^2; K is the rock thermal conductivity, W/(m·K); and G is the geothermal gradient, °C/km. The negative sign (-) indicates that heat flow changes from the interior of the Earth to the surface.

The geothermal gradient is one of the important key parameters in the Equation 1. In this study, the geothermal gradient was calculated by Equation 2 using the SSSTD measurements (Fig. 4).

$$G=(T_2-T_1)/(Z_2-Z_1) \tag{2}$$

where G is the geothermal gradient of the stratum, °C/km; T_1 and T_2 (°C) are the stratum temperatures corresponding to burial depths Z_1 and Z_2 (km), respectively.

3.2 Basic parameters

3.2.1 System steady-state temperature data

A total of 193 system steady-state temperature data of the Wells X2, X5, Y5 and Y7 were tested and obtained (Tables 1-4). The Wells X2, X5 and Y5 are located in the Wuliji fault-nose structural zone, and the Well Y7 is located in the central structural zone. The formation temperatures from the Bayingebi 2 Formation to the Cenozoic were tested in the Wells X2, X5 and Y7, and the formation temperatures from the Suhongtu Formation to the Cenozoic were tested in the Well Y5. Since the Cenozoic is affected by these factors such as solar radiation and groundwater disturbance, the formation temperatures of the Cenozoic were not considered during the calculation.

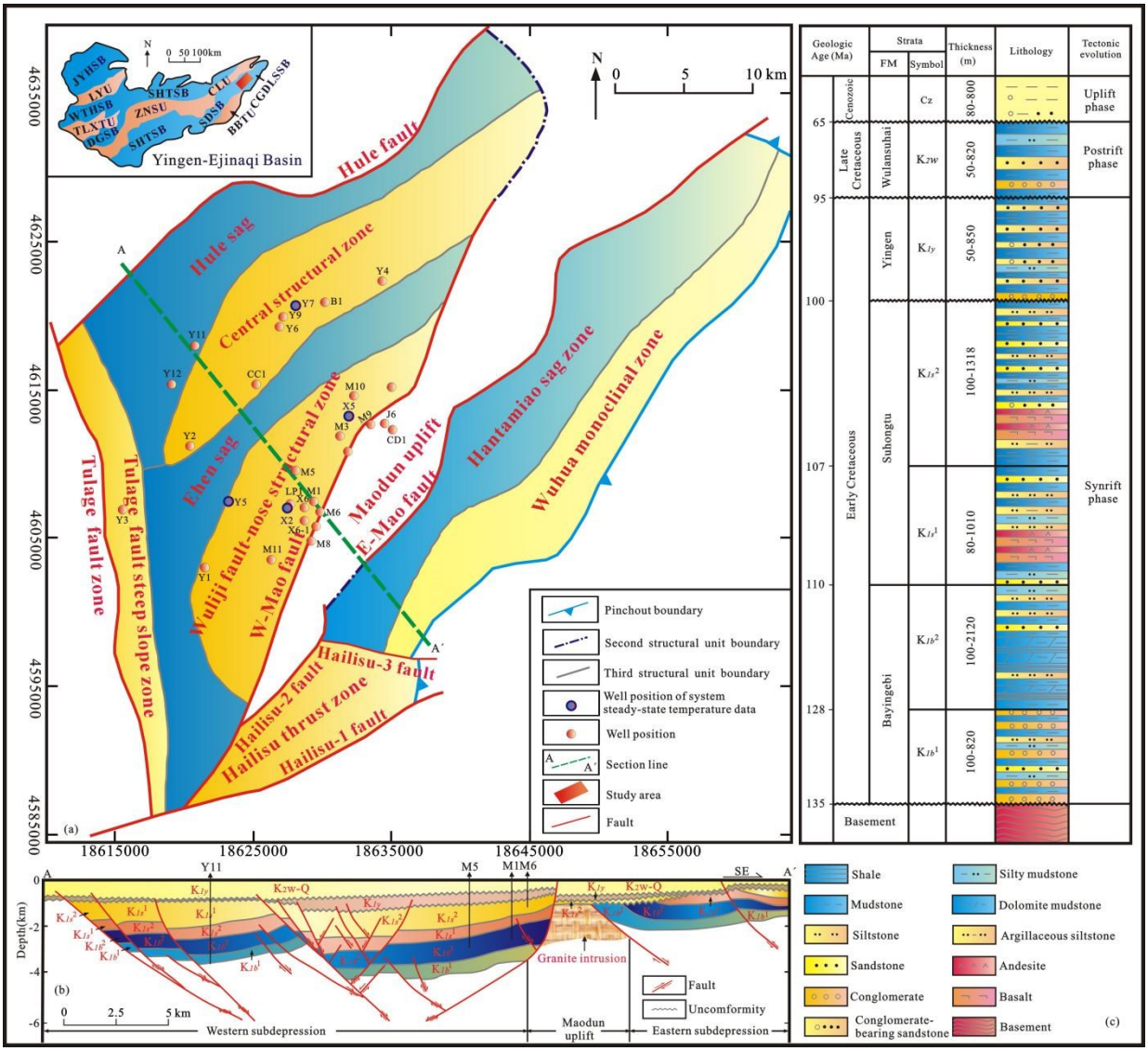

Figure 2: (a) Structural unit division of the Chagan Depression; (b) Structural profile; (c) Stratigraphic column.
Abbreviatios: JYHSB: Juyanhai subbasin; LYU: Lüyuan uplift; WTHSB: Wutaohe subbasin; TLXTU: Teluoxitan uplift; SHTSB: Suhongtu subbasin; DGSB: Dagu subbasin; ZNSU: Zongnasishan uplift; SHTSB: Suhetu subbasin; SDSB: Shangdan subbasin; BBTU: Benbata uplift; CGDLSSB: Chagandelesu subbasin; CLU: Chulu uplift.

3.2.2 Rock thermal conductivity

The Upper Cretaceous and Cenozoic in the Chagan Depression are not the targeted layers for oil and gas exploration, therefore there are no core samples. Based on the original rock thermal conductivity data (Zuo et al., 2013b), the rock thermal conductivity data of 62 samples of the Wells Y7, Y5 and X5 were newly measured. There are 169 rocks thermal conductivity data in total. Their lithology is mainly mudstone, sandstone and volcanic rock. Here, the new rock thermal conductivity data of 62 rock samples were measured at the Geothermal and Environmental Research Institute of Xi'an Jiaotong University.

4. RESULTS

4.1 Rock thermal conductivity

The rock thermal conductivity data in the Chagan Depression are concentrated in 1.5~3.0 W/(m·K). On the whole, they have a slight increase with the increase of depths. Considering the lithology only, the rock thermal conductivity data of sandstone and magmatic rocks increase with the increase of depth, but the change in the rock thermal conductivity data of mudstone are not obvious.

According to the percentage of sandstone, mudstone, and magmatic rock in 21 wells, the thermal conductivity of different strata were obtained by Equation 3, and the average value is 2.11 ± 0.28 W/(m·K) (Table 5).

$$K = K_sP_s + K_nP_n + K_mP_m \quad (3)$$

where *Ks*, *Kn*, and *Km* are the thermal conductivity data for sandstone, mudstone, and magmatic rock, W/(m·K); P_s, P_n, and P_m are the percentages of sandstone, mudstone, and magmatic rock, %.

Table 1: System stable-state temperature data of the Well X2 in the Chagan Depression.

No.	Temperature (℃)	Depth (m)	Strata	No.	Temperature (℃)	Depth (m)	Strata
1	26.34	0	Cenozoic	33	40.33	1238	K_1s^2
2	25.76	9	Cenozoic	34	41.89	1291	K_1s^2
3	24.62	58	Cenozoic	35	43.19	1339	K_1s^2
4	23.68	102	Cenozoic	36	44.49	1385	K_1s^2
5	22.93	145	Cenozoic	37	46.14	1438	K_1s^2
6	21.99	201	Cenozoic	38	47.75	1494	K_1s^2
7	21.43	248	Cenozoic	39	49.87	1558	K_1s^2
8	20.90	299	Cenozoic	40	51.43	1595	K_1s^2
9	20.39	322	Cenozoic	41	53.94	1655	K_1s^2
10	20.20	352	Cenozoic	42	56.02	1704	K_1s^2
11	20.38	369	Cenozoic	43	58.45	1762	K_1s^2
12	20.81	419	Cenozoic	44	59.06	1776	K_1s^2
13	21.42	472	Cenozoic	45	60.79	1819	K_1s^2
14	21.80	511	K_2w	46	63.48	1884	K_1s^2
15	22.63	556	K_2w	47	64.82	1919	K_1s^2
16	23.68	606	K_2w	48	67.04	1975	K_1s^1
17	24.80	654	K_2w	49	68.77	2038	K_1s^1
18	25.75	692	K_1y	50	69.99	2079	K_1s^1
19	26.69	732	K_1y	51	71.20	2118	K_1s^1
20	27.49	763	K_1y	52	72.73	2156	K_1s^1
21	28.28	809	K_1y	53	74.42	2205	K_1s^1
22	28.85	837	K_1y	54	76.30	2257	K_1s^1
23	29.14	858	K_1y	55	78.40	2316	K_1s^1
24	30.27	903	K_1y	56	80.39	2370	K_1s^1
25	31.01	939	K_1y	57	82.21	2420	K_1s^1
26	31.76	975	K_1y	58	84.56	2485	K_1s^1
27	33.08	1035	K_1y	59	86.90	2545	K_1s^1
28	34.02	1075	K_1y	60	89.15	2604	K_1s^1
29	34.86	1112	K_1y	61	91.75	2698	K_1b^2
30	36.68	1118	K_1y	62	93.66	2765	K_1b^2
31	38.24	1167	K_1y	63	94.58	2800	K_1b^2
32	38.85	1192	K_1y				

Table 2: System steady-state temperature data of the Well X5 in the Chagan Depression

No.	Temperature (℃)	Depth (m)	Strata	No.	Temperature (℃)	Depth (m)	Strata
1	24.69	1	Cenozoic	19	33.17	986	K_1s^2
2	23.93	16	Cenozoic	20	33.94	1012	K_1s^2
3	22.11	61	Cenozoic	21	35.09	1051	K_1s^2
4	20.51	109	Cenozoic	22	36.44	1100	K_1s^2
5	16.58	150	Cenozoic	23	38.02	1157	K_1s^2
6	13.03	183	Cenozoic	24	40.05	1197	K_1s^2

7	16.89	352	Cenozoic	25	44.78	1301	K_1s^2
8	18.41	396	Cenozoic	26	47.49	1365	K_1s^2
9	20.07	448	Cenozoic	27	51.36	1452	K_1s^2
10	21.75	512	K_1y	28	53.00	1491	K_1s^2
11	23.75	597	K_1y	29	56.08	1563	K_1s^2
12	25.20	657	K_1y	30	60.61	1670	K_1s^2
13	26.45	711	K_1y	31	64.27	1760	K_1s^1
14	26.73	721	K_1y	32	69.81	1900	K_1s^1
15	27.75	762	K_1y	33	71.39	1946	K_1s^1
16	29.48	830	K_1y	34	75.68	2060	K_1s^1
17	30.45	880	K_1s^2	35	78.95	2165	K_1b^2
18	31.82	931	K_1s^2	36	80.97	2242	K_1b^2

Table 3: System steady-state temperature data of the Well Y5 in the Chagan Depression

No.	Temperature (℃)	Depth (m)	Strata	No.	Temperature (℃)	Depth (m)	Strata
1	22.70	10	Cenozoic	26	54.67	1735	K_1s^2
2	18.74	51	Cenozoic	27	55.72	1771	K_1s^2
3	16.48	111	Cenozoic	28	56.85	1808	K_1s^2
4	15.69	150	Cenozoic	29	58.12	1858	K_1s^2
5	15.36	196	Cenozoic	30	59.38	1903	K_1s^2
6	15.43	242	Cenozoic	31	62.63	1975	K_1s^2
7	15.43	283	Cenozoic	32	64.60	2020	K_1s^2
8	15.78	315	Cenozoic	33	66.71	2069	K_1s^2
9	16.54	376	Cenozoic	34	68.12	2106	K_1s^2
10	17.01	426	Cenozoic	35	71.22	2180	K_1s^2
11	17.64	453	Cenozoic	36	72.77	2224	K_1s^2
12	18.70	500	Cenozoic	37	75.31	2290	K_1s^2
13	22.35	629	K_2w	38	76.58	2324	K_1s^2
14	26.29	729	K_2w	39	78.27	2365	K_1s^2
15	28.77	798	K_2w	40	80.34	2416	K_1s^2
16	31.48	885	K_2w	41	82.36	2466	K_1s^1
17	34.38	988	K_2w	42	84.19	2516	K_1s^1
18	36.83	1088	K_2w	43	87.15	2590	K_1s^1
19	38.40	1152	K_2w	44	89.12	2638	K_1s^1
20	41.20	1253	K_1y	45	91.38	2700	K_1s^1
21	44.04	1358	K_1y	46	93.07	2747	K_1s^1
22	46.84	1472	K_1y	47	95.32	2811	K_1s^1
23	49.38	1548	K_1s^2	48	97.15	2865	K_1s^1
24	51.07	1608	K_1s^2	49	97.80	2899	K_1s^1
25	52.76	1668	K_1s^2				

Table 4: System steady-state temperature data of the Well Y7 in the Chagan Depression

No.	Temperature (℃)	Depth (m)	Strata	No.	Temperature (℃)	Depth (m)	Strata
1	9.17	3	Cenozoic	24	41.72	1132	K_1s^2
2	9.36	33	Cenozoic	25	45.01	1217	K_1s^2
3	10.06	77	Cenozoic	26	46.04	1246	K_1s^2
4	11.09	130	Cenozoic	27	48.70	1328	K_1s^2
5	12.50	191	Cenozoic	28	51.77	1400	K_1s^2
6	13.86	251	Cenozoic	29	53.18	1433	K_1s^2
7	15.32	311	Cenozoic	30	54.22	1458	K_1s^2
8	16.63	361	Cenozoic	31	55.63	1490	K_1s^2
9	18.12	411	Cenozoic	32	56.76	1512	K_1s^2
10	18.79	439	Cenozoic	33	58.44	1559	K_1s^1
11	20.49	493	Cenozoic	34	60.32	1612	K_1s^1
12	22.46	544	K_2w	35	62.20	1671	K_1s^1

13	24.43	602	K_2w	36	64.08	1725	K_1s^1
14	26.03	657	K_2w	37	65.96	1775	K_1s^1
15	28.27	733	K_2w	38	67.84	1826	K_1s^1
16	28.96	755	K_2w	39	69.34	1878	K_1s^1
17	29.74	780	K_2w	40	70.53	1916	K_1s^1
18	31.67	840	K_2w	41	72.35	1970	K_1s^1
19	33.36	889	K_1y	42	74.73	2036	K_1s^1
20	35.43	939	K_1s^2	43	76.01	2080	K_1b^2
21	36.94	994	K_1s^2	44	77.24	2125	K_1b^2
22	38.62	1045	K_1s^2	45	78.93	2184	K_1b^2
23	40.03	1090	K_1s^2				

4.2 Present gradient and terrestrial heat flow

The relationships between the SSSTD and the depths from four wells in the Chagan Depression is shown in three sections (Figure 3). The average geothermal gradients from the upper section to the lower section are 28.9, 37.6 and 27.6 °C/km (Table 6). The low geothermal gradient in the upper section may be affected by groundwater or residual liquid in oil wells. Moreover, the upper section mainly includes the upper part of the Suhongtu 2 Formation, the Yingen Formation, the Sulansuhai Formation and the Cenozoic deposits and rock thermal conductivity data are few, because of the lack of core samples in the upper section. Therefore, the SSSTD of the upper section cannot be used to calculate the terrestrial heat flow. Furthermore, this article focuses on the middle and lower sections to calculate the geothermal gradient and terrestrial heat flow. The results show that the geothermal gradient in the middle section is higher than the geothermal gradient in the lower section, showing negative correlation with the rock thermal conductivity. In general, the geothermal gradient of the Chagan Depression ranges from 31.5 °C/km (Well Y7) to 33.6 °C/km (Well X5), with an average value of 32.6 °C/km (Table 6).

Table 5: Rock thermal conductivity (K) for strata in the Chagan Depression

Strata	Lothlogy	Sample numbers	K_{range} [W/(m·K)]	$K_{average}$ ± standard deviation [W/(m·K)]	Content of lithology (%)	K_{strata} [W/(m·K)]
K_1y	Mudstone	3	1.91-2.00	1.96±0.05	49.1	1.85
	Sandstone	7	1.14-2.49	1.75±0.40	50.9	
K_1s^2	Mudstone	3	1.58-1.79	1.69±0.11	55.2	1.78
	Sandstone	8	2.04-2.40	2.17±0.14	22.6	
	Magmatic rock	15	0.86-3.01	1.59±0.52	22.3	
K_1s^1	Mudstone	28	1.81-3.64	2.28±0.40	53.6	2.21
	Sandstone	20	1.64-3.23	2.49±0.40	22.7	
	Magmatic rock	10	1.36-2.17	1.78±0.25	23.7	
K_1b^2	Mudstone	36	1.46-2.81	2.19±0.29	70.1	2.33
	Sandstone	28	1.92-3.45	2.65±0.40	29.9	
K_1b^1	Mudstone	4	1.78-2.44	2.11±0.27	61.0	2.38
	Sandstone	7	2.50-3.26	2.80±0.20	39.0	

$\sigma = \sqrt{\frac{1}{N}\sum_{i=1}^{N}(x_i-\mu)^2}$ σ is the standard deviation; N is the number of rock samples; χ_i is the rock thermal conductivity of a rock sample; μ is the arithmetic mean; K is the rock thermal conductivity.

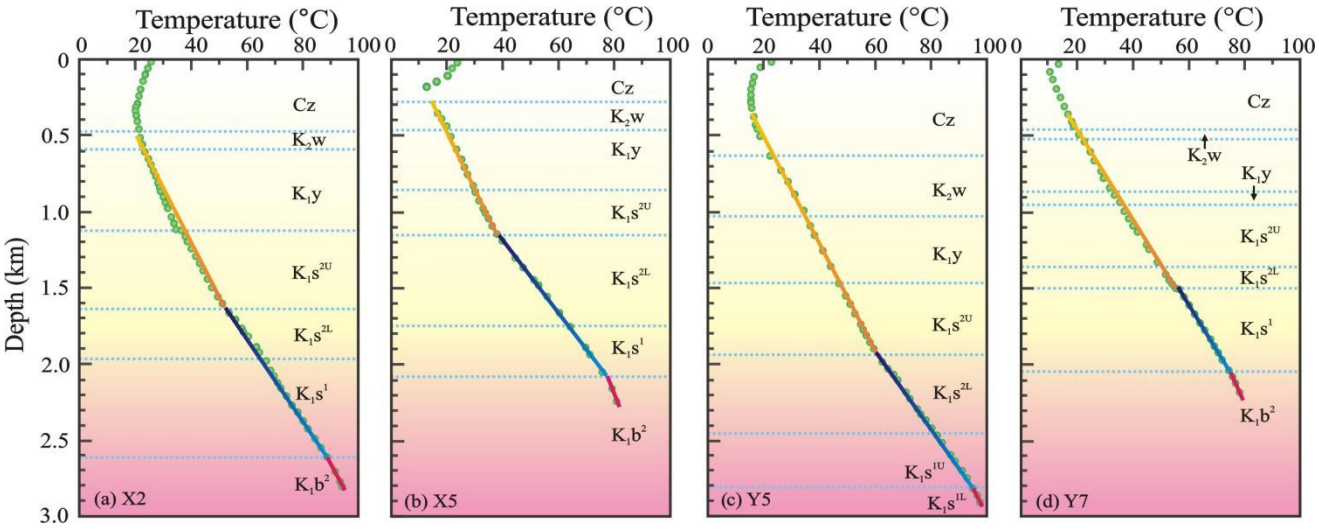

Figure 3: System steady-state temperature data measurements for typical wells in the Chagan Depression

According to the rock thermal conductivity and the geothermal gradient data, the terrestrial heat flows of four wells are calculated using thermal resistance methods (Chapman, 1984). The terrestrial heat flow of the Chagan Depression ranges from 67.3 mW/m^2 to 71.0 mW/m^2, with an average value of 68.9 W/m^2 (Table 6). This value indicates high terrestrial heat flow and is higher than the global continental average terrestrial heat flow of 63.0 mW/m^2 (Wang et al., 2015).

5. HEAT FLOW STATE AND TECTONIC SETTINGS

Previous studies have shown that the YE Basin has a craton-type lithospheric structure with low terrestrial heat flow and mantle heat flow, as well as large lithospheric thickness, and that it is a stable tectonic zone (Wang and Huang, 1988, 1990; Hu et al., 2000; Wang, 2015). However, this study reveals that the Chagan Depression has a high terrestrial heat flow, ranging from 67.3 to 71.0 mW/m^2, with an average value of 69.0 mW/m^2 (Table 6).

Table 6: Geothermal gradient (G) and terrestrial heat flow (q) data in the Chagan Depression

Well	Latitude	Longitude	Depth range (m)	Strata range	G (°C/km)	K [W/(m·K)]	q_{strata} (mW/m^2)	$q_{average}$ (mW/m^2)
X2	41°35′13″N	106°31′44″E	500-1650	K_2w-K_1s^{2U}	27.7	-	-	68.4
			1650-2617	K_1s^{2L}-K_1s^1	36.2	1.98	71.7	
			2617-2800	K_1b^2	27.9	2.33	65.0	
X5	41°38′34″N	106°35′03″E	298-1300	K2w-K_1s^{2U}	25.8	-	-	71.0
			1300-2090	K_1s^{2L}-K_1s^1	40.9	1.98	81.0	
			2090-2242	K_1b^2	26.2	2.33	61.0	
Y5	41°35′27″N	106°28′32″E	380-2000	K_2w-K_1s^{2U}	28.4	-	-	69.1
			2000-2811	K_1s^{2L}-K_1s^{1U}	38.3	1.98	75.8	
			2811-2899	K_1s^{1L}	28.2	2.21	62.3	
Y7	41°42′45″N	106°32′29″E	360-1500	Cz-K_1s^{2U}	33.6	-	-	67.3
			1500-2040	K_1s^{2L}-K_1s^1	34.9	1.98	69.1	
			2040-2184	K_1b^2	28.1	2.33	65.5	

Terrestrial heat flow is an objective reflection of the dynamics of the sedimentary basin and the thermal evolution of the lithospheric structure. Sedimentary basins of different ages and different origins show obvious differences in their present-day thermal states. For areas with stable basement, the terrestrial heat flow is low, such as Precambrian shield areas with terrestrial heat

flow of approximately 41.8 mW/m^2 (Irina, 2006). For tectonically active areas, terrestrial heat flow is high, such as areas of Cenozoic tectonic activity area: the American Basin and Range region with a terrestrial heat flow of approximately 83.0 mW/m^2 (Morgan, 1982), the modern continental marginal expansion basin, the South China Basin, with a terrestrial heat flow of approximately 78.3 mW/m^2 (He et al., 1998); and the modern continental rift, Baikal Rift, with a terrestrial heat flow of approximately 99.0 mW/m^2 (Morgan, 1982).

The average terrestrial heat flow in the Chagan Depression is 69.0 mW/m^2, which confirms that the Chagan Depression has not only a high heat flow state (Zuo et al., 2015), but also a geothermal state between the a tectonically active zone and a tectonically stable zone.

The Moho depth of the Yingen-Ejinaqi Basin is 41.5 km (Meng et al., 1995), and it is shallower than the Moho depth of the Tarim Basin and the Qaidam Basin in the west, and deeper than those in the North China Basin and the Liaohe Basin in the east (Qiu, 1998). However, the terrestrial heat flow in the Yingen-Ejinaqi Basin is larger than in these above basins. The reason is that the Yingen-Ejinaqi Basin is formed by the extension of the Altun Fault to the northeast direction in the Early Cretaceous, and the strike-slip fault cut into the upper mantle of the lithosphere (Che et al., 1998; Xu et al., 1999). This series of movements were accompanied by magma spurting and large tensile stresses and thinning of the lithosphere during the formation of the basin, and caused the mantle material to surge and brought a lot of heat. The Early Cretaceous had exhibited the highest geothermal background. The current heat flow on the surface still shows the Cretaceous heat state, but the heat flow is declining.

The basement of the Yingen-Ejinaqi Basin is an island-arc fold belt, and it was formed at the intersection of the North China Plate, the Tarim Plate, and the Kazakhstan Plate during the Paleozoic. It has the properties of the Paleozoic orogenic belt (Wu and He, 1993). Some Meso-Cenozoic basins were developed on this orogenic belt and between the deep faults or the Paleo-subduction zones and the Paleo-suture zones, and the current constructions are very complicated. Since the Paleogene, the northward subduction of the Indian plate collided with the Eurasian plate, and the Indian plate is still moving to the Eurasian plate at a very slow speed. The Yingen-Ejinaqi Basin has been continuously squeezed by the collision of these two plates. These movements cause the southwestern boundary of the basin to migrate northward, and it is still happening continuously (Yang, 2011). Meanwhile, the southeastern part of the basin is subject to the NWW-trending subduction of the Pacific Plate, and it causes the southeast boundary of the basin to migrate northward. At the same time, the Siberia Plate blocks the northward movement of the Yingen-Ejinaqi Basin (Chen, 1994). Under the complicated tectonism, the basin is still in a higher thermal state. Some reverse faults and folds were found in the Shangdan depression and the Chagandulesu depression, but the tectonic movement intensity was not as strong as in the modern continental margin expansion basin and the Cenozoic tectonic activity zone. The results show the Yingen-Ejinaqi Basin is now in a tectonic setting between tectonically stable and active areas, and it is consistent with the geothermal state revealed by the geothermal flow in the Chagan Depression.

6. CONCLUSIONS

(1) The average rock thermal conductivity of the Chagan Depression is 2.11 ± 0.28 W/(m·K). the geothermal gradient of the Chagan Depression ranges from 31.5 °C/km (Well Y7) to 33.6 °C/km (Well X5), with an average value of 32.6 °C/km. The segmentation of the geothermal gradient is mainly due to differences of the rock thermal conductivities in the different strata;

(2) The Chagan Depression has a high terrestrial heat flow background, ranging from 67.3 to 71.0 mW/m^2 with an average value of 69.0 mW/m^2, and its geothermal state is intermediate between a tectonically active zone and a tectonically stable zone.

ACKNOWLEDGEMENTS

This work was funded by the Foundation of State Key Laboratory of Petroleum Resources and Prospecting, China University of Petroleum, Beijing (Grant No. PRP/open-1705), Sichuan Science & Technology Foundation (Grant No. 2016JQ0043), Geoscience Young Science Foundation of Liu Baojun (Grant No. DMSM2017003), National Natural Science Foundation of China (Grant No. 41402219) and National Basic Research Program of China (Grant No. 2016ZX05006-004).

REFERENCES

Artemieva, I.M.: Lithosphere structure in Europe from thermal isostasy, *Earth-Science Reviews*, 188, (2018), 454-468.

Che, Z.C., Liu, L., Liu, H.F., and Luo, J.H.: The constituents of the Altun fault system and genetic characteristics of related Meso–Cenozoic petroleum–bearing basin, *Geological Bulletin of China*, 17(4), (1998), 377–384 (in Chinese with English abstract).

Chen, C.C.: A personal view on rotation drift movement of the Siberia plate. *World Regional Studies*, 1, (1994), 67–71 (in Chinese).

He, L.J., Xiong, L.P., and Wang, J.Y.: The geothermal characteristics in South China Sea, *China Offshore Oil and Gas (Geology)* 13(2), (1998), 87–90 (in Chinese with English abstract).

Hu, S.B., He, L.J., and Wang, J.Y.: Heat flow in the continental area of China: a new data set, *Earth ans Planetary Science Letters*, 179, (2000), 407–419.

Irina, M.A.: Global 1°×1° thermal model TC1 for the continental lithosphere Implications for lithosphere secular evolution, *Tectonophysics*, 416, (2006), 245–277.

Lu, J.C., Zhang, H.A., Niu, Y.Z., Liu, F.C., Chen, Q.T., and Wei, J.S.: Carboniferous-Permian petroleum conditions and exploration breakthrough in the Yingen-Ejin Basin in Inner Mongolia, *Geology in China*, 44(1), (2017), 13–32 (in Chinese with English abstract).

Majorowicz, J. A., Grad, M., and Polkowski, M.: Terrestrial heat flow versus crustal thickness and topography–European continental study, *International Journal of Terrestrial Heat Flow and Applications*, 2(1), (2019), 17–21.

Meng, L.S., Guan, Y., Qi, L., and Gao, R.: Gravity field and deep crustal structure in Golmud–Ejin Qi geoscience transection and nearby area, *Chinese Journal of Geophysics*, 38(S2), (1995), 36–45 (in Chinese with English abstract).

Morgan, P.: Heat flow in rift zones, *American Geophysical Union*, (1982), 107–122.

Qiu, N.S.: Thermal status profile in terrestrial sedimentary basins in China, *Advances in Earth Sciences*, 13(5), (1998), 447–451 (in Chinese with English abstract).

Ren, J.S.: Tectonic map of China and adjacent regions, Beijing: Geological Publishing House, (1999).

Wan, T.F.: The Tectonics of China - Data, Maps and Evolution, Springer-Verlag Berlin Heidelberg, (2011).

Wang, J.Y.: Geothermal and its application. Beijing: Science Press (2015) (in Chinese).

Wang, J.Y., and Huang, S.P.: Compilation of heat flow data foe continental area of China, *Scientia Geologica Sinica*, 31(2), (1988), 196-204 (in Chinese with English abstract).

Wang, J.Y., and Huang, S.P.: Compilation of heat flow data foe continental area of China (2nd editor), *Seismology and Geology*, 12(4), (1990), 351-366 (in Chinese with English abstract).

Wang, S.L., Shi, P., Zhang, F.D., and Qi, R.L.: Petroleum geologic features and exploration discovery in Chagan sag, China *Petroleum Exploration*, 21(3), (2016), 108–115 (in Chinese with English abstract).

Wei, P.S., Zhang, H.Q., and Chen, Q.L.: Petroleum geological characteristics and exploration prospects in the Yingen–Ejinaqi Basin, Beijing: Petroleum Industry Press (2006) (in Chinese).

Wu, T.R., and He, G.Q.: Tectonic units and their fundamental characteristics on the northern margin of the Alxa block, *Acta Geologica Sinica*, 67(2), (1993), 97–108 (in Chinese with English abstract).

Xu, Z.Q., Yang, J.S., Zhang, J.X., Jiang, M., Li, H.B., and Cui, J.W.: A comparison between the tectonic units on the two sides of the Altun sinistral strike-slip fault and the mechanism of lithospheric shearing, *Acta Geologica Sinica*, 73(3), (1999), 193–205 (in Chinese with English abstract).

Yang, J.L.: Discussion on intraland plate moving evolvement in China and the relationship with earthquake, *Inland Earthquake*, 25(2), (2011), 109–119 (in Chinese with English abstract).

Zhong, F.P., Zhong, J.H., Wang, Y., and You, W.F.: Geochemistry characteristics and origin of Early Cretaceous volcanic rocks in Suhongtu Depression, Inner Mongolia, China, *Acta Mineralogica Sinica*, 34(1), (2014), 107–116 (in Chinese with English abstract).

Zuo, Y.H., Qiu, N.S., Deng, Y.X., Rao, S., Xu, S.M., and Li, J.G.: Terrestrial heat flow in the Qagan sag, Inner Mongolia, *Chinese Journal of Geophysics*, 56(9), (2013), 3038–3050 (in Chinese with English abstract).

Zuo, Y.H., Qiu, N.S., Hao, Q.Q., Pang, X.Q., Gao, X., Wang, X.J., Luo, X.P., and Zhao, Z.Y.: Geothermal regime and source rock thermal evolution history in the Chagan Depression, Inner Mongolia. *Marine and petroleum Geology*, 59(1), (2015), 245–267.

Zuo, Y.H., Song, R.C., Li, Z.X., Wang, Y.X., and Yang, M.H.: Lower Cretaceous source rock evaluation and thermal maturity evolution of the Chagan depression, Inner Mongolia, Northern China, *Energy Exploration & Exploitation*, 35(4), (2017), 482–503.